Determination of 4-nitrophenol in Water using Free-Standing Cu Nanowire Electrode

Xiaoping Zhang, Lingxiao Chen, Yifan Zheng, Haodong Tang, Zongjian Liu[*]

Institute of Industrial Catalysis, College of Chemical Engineering, Zhejiang University of Technology, Hangzhou 300014, P.R. China
[*]E-mail: zjliu@zjut.edu.cn

While Au and Ag are widely used as the electrocatalysts for sensing 4-nitrophenol (4-NP), Cu is seldom studied probably due to the fact that its performance is not as good as those of Au and Ag. In this work, the electrocatalytic activity of a free-standing Cu nanowire (CuNW) electrode for 4-NP reduction, as well as its performance as a sensor for detection of 4-NP in water, has been studied. The electrochemical impedance spectroscopy analysis indicates that, owing to its a porous network structure with CuNWs serving as both conductive substrate and electrocatalyst, the free-standing CuNW electrode possesses a much lower electron transfer resistance and a much higher electrochemical active surface area than a CuNW-modified glassy carbon electrode (GCE). A comparative study on the electroreduction of 4-NP at different Cu electrodes by cyclic voltammetry (CV) reveals that no reduction peak appears at a Cu wire electrode with low active surface area but fast charge transfer while a broad peak is observed at the CuNW-modified GCE with slow charge transfer but relatively higher active surface area. Benefitting from the combination of fast electron transfer and high active surface area, however, the 4-NP reduction peak at the free-standing CuNW electrode is narrow and positively shifted with its current being more than 30 times higher than that observed at the CuNW-modified GCE. These features allow an investigation of this free-standing CuNW electrode as a 4-NP sensor via a simple electrochemical technique (namely CV), and the results obtained demonstrate that this sensor exhibits a linear range of 4 to 2200 μM, a sensitivity of 4.831 μA/μM, and a detection limit of 1.0 μM at a signal-to-noise ratio of 3. Compared with the reported porous Cu-modified graphite pencil electrode, our Cu-based 4-NP sensor not only possesses a lower detection limit but also has a much broader linear range and higher sensitivity.

1. INTRODUCTION

4-Nitrophenol (4-NP) is widely used as a raw material or intermediate to produce pharmaceuticals, pesticides and dyes. The extensive use of 4-NP, however, has resulted in an increasing discharge of 4-NP-bearing wastewater and thus aroused an environmental concern due to its

high resistance to biological degradation and toxic effect on humans, animals and plants [1-4]. 4-NP can, for example, irreversibly damage the liver, kidneys and other organs of animals and humans [4]. In view of its water-soluble nature and strong toxicity, monitoring the concentration of 4-NP in water is of great importance.

The concentration of 4-NP can be determined by a number of analytical methods, such as spectroscopy [5], chromatography [6], fluorescence [7] and electrochemical techniques [8-10]. Among these methods, the electrochemical method based on the reduction of 4-NP at the cathode has drawn great attention due to its simplicity, low cost and quick response [8-17]. Since the performance of a 4-NP electrochemical sensor depends heavily on the cathode used, the choice of a suitable electrode material is of great importance. Noble metals, e.g. Au and Ag, are commonly used as the electrocatalysts for sensing 4-NP due to their excellent electrocatalytic activity for reduction of 4-NP [9-12]. To improve the performance of Au or Ag based 4-NP sensors, various Au or Ag based composites have recently been developed, including Au-graphene [13], Au-reduced graphene oxide (RGO) [14], Ag-multilayer carbon nanotube (MCNT) [15] and Ag-RGO [16]. On the contrary, despite that Cu has been found to be a good catalyst for reduction of 4-NP in the presence of $NaBH_4$ [18], this non-noble metal was seldom used as the 4-NP electrochemical sensor in the past probably due to the fact that the performance of the reported Cu-based 4-NP sensors, e.g. porous Cu-modified graphite pencil electrode (GPE) [17], are not as good as those of Au or Ag based sensors.

In this article, we report a study on the electroreduction and detection of 4-NP in water at a free-standing Cu nanowire (CuNW) electrode, with a CuNW-modified glassy carbon electrode (CuNW/GCE) being investigated for comparison. Interest in this work is based on the following considerations. (i) The free-standing CuNW electrode (F-CuNWE) fabricated by thermal annealing of CuNWs owns a high active surface area [19] and thus has the advantage over the modified electrodes that often offer a low active surface area. Despite the fact that Au and Ag are generally more active than Cu in the electroreduction of 4-NP, the F-CuNWE might exhibit a performance that can be comparable to those of Au and Ag based sensors because these sensors are normally based on the modified electrodes. (ii) In the F-CuNWE, CuNWs serve as both conductive substrate and electrocatalyst, which is different from the modified electrodes where the electrocatalysts are decorated on a conductive substrate. A fast charge transfer is therefore assumed at the free-standing electrode due to the absence of both the substrate-electrocatalyst interface and the polymer binder, but no work provides evidence for this speculation. (iii) Although the free-standing electrode has above-mentioned advantages over the modified electrode, how these advantages affects the electroreduction of 4-NP is unknown. Therefore, the present work focuses on the difference in electron transfer between F-CuNWE and CuNW/GCE, the effect of both electron transfer resistance and active surface area on the electroreduction of 4-NP at the electrodes and the performance of the F-CuNWE as a 4-NP sensor.

2. EXPERIMENTAL

All chemicals were of analytical grade and used as received without further purification. Double-distilled water was used for preparing all solutions. CuNWs used in the experiments were synthesized via a cheap and environmentally friendly method developed by our group [21].

To prepare the F-CuNWE, a mould was first filled with a dense CuNW slurry obtained by dispersing CuNW into ethanol (see Step 1 in Fig. 1). After dried in N_2 atmosphere at 70^oC, the mould was removed and the obtained CuNW film was connected with a Cu wire (see Steps 2 and 3 in Fig. 1). Then, the CuNW film was annealed under Ar atmosphere at 600^oC for 30 min. Finally, the Cu wire was sealed with epoxy resin to obtain an F-CuNWE of about $0.5 \times 0.6 \times 0.05$ cm^3 in size (see Step 4 in Fig. 1). For comparison, a CuNW/GCE was also prepared according to the following procedure. First of all, a bare GCE with a diameter of 3 mm was polished with alumina slurries (1µm and 0.05µm) and then ultrasonicated successively in acetone, ethanol and deionised water, followed by dried at room temperature. Secondly, 15 mg of CuNWs was dispersed into 1 mL of water. And then, 90 µL of chitosan solution (1 wt.%, pH=5), which served as a binder, was added into the above CuNW-water mixture and then ultrasonicated to achieve a dispersion. Finally, a CuNW/GCE was obtained by drop-casting 20 µL of the resulting dispersion onto the pretreated GCE and then dried at room temperature.

The surface morphology of the samples was examined by scanning electron microscope (SEM, Hitachi S-4700) operating at 15 kV. Electrochemical measurements were conducted at room temperature with a CHI660E workstation (CHI Instruments). The setup was a conventional three-electrode cell with a platinum wire as counter electrode and a saturated calomel electrode (SCE) as reference electrode. Unless otherwise stated, all measurements were conducted in 0.15 M acetate buffer solution with a pH value of 5. Before measurement, N_2 purging was performed to remove the oxygen from the electrolyte solution. Spectrometric measurement was performed on a UV-vis 7600 spectrophotometer (Shanghai Jinghua Instrument) at room temperature. The sample cells were rectangular quartz cuvettes with 1 cm path length. The absorption spectra of both standard solutions and unknown samples were obtained in the range of 190–1100 nm with 1 nm resolution. For the unknown high-concentration sample whose absorbance was beyond the linear range of the calibration curve, a dilution was needed prior to the measurement.
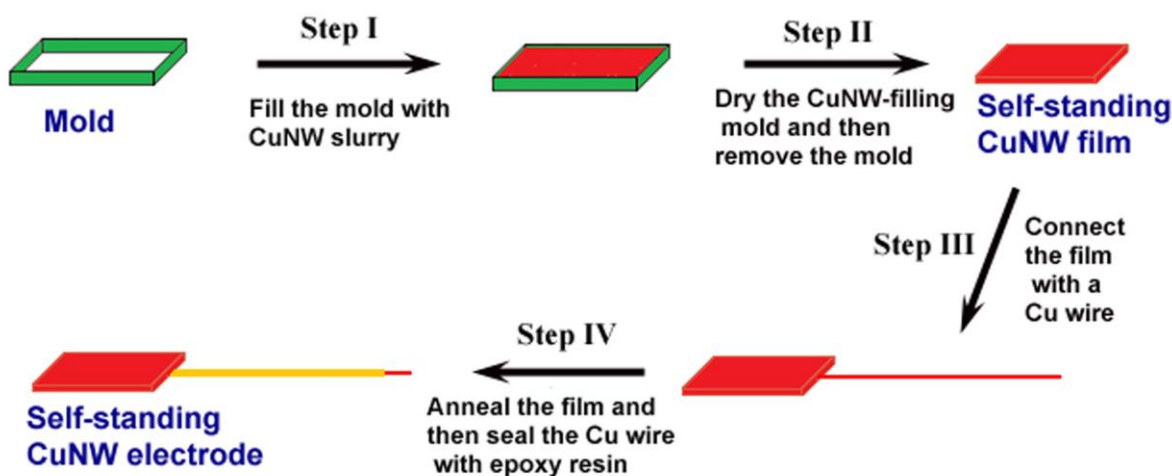

Figure 1. Schematic illustration for preparation of F-CuNWE.

3. RESULTS AND DISCUSSION

3.1 Characterization of CuNW-based electrodes

Our previous study has revealed that thermal annealing of a CuNW film at 600°C can achieve an F-CuNWE of good physical stability [19]. Although a modification on the preparation of the CuNW film is made in this work, the morphology of the unannealed film (Fig. 2a) or the resulting F-CuNWE (Fig. 2b) is similar to that observed in our previous work [19]. It is obvious that the F-CuNWE owns a porous network structure resulting from the melting of CuNWs, as is evident from the change in nanowire size after annealing. Benefitting from its porous network structure, the as-formed F-CuNWE can offer an electrochemical active surface area 200 times higher than that of a Cu wire electrode having nearly the same geometrical area as the F-CuNWE [19]. On the contrary, the change in nanowire size cannot be found in the CuNW/GCE, but the polymer binder can be observed on the surface of some CuNWs (Fig. 2c). Undoubtedly, the use of polymer binder in preparation of CuNW/GCE will not only block the catalytic active sites but also increase the electron transfer resistance.
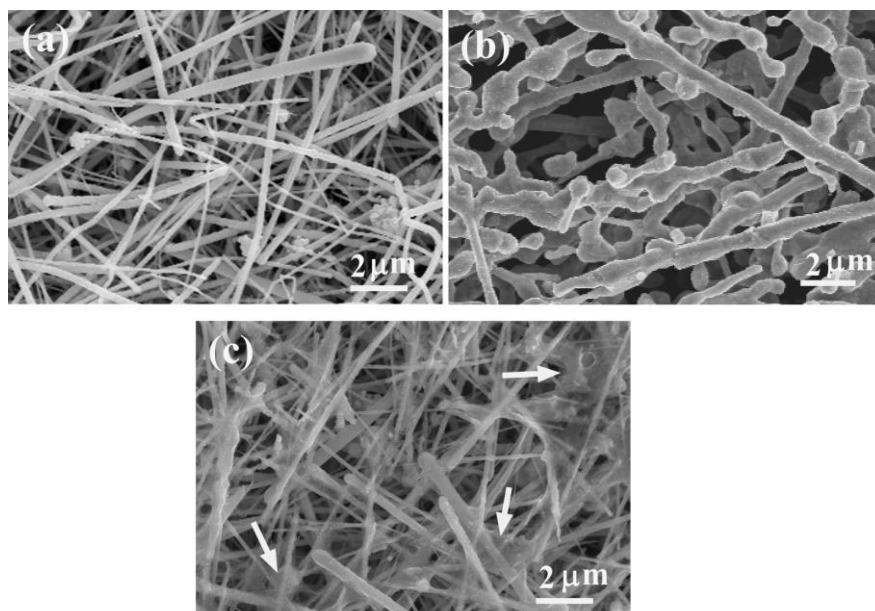

Figure 2. SEM images of (a) CuNW film before annealing, (b) CuNW film after annealing, and (c) the binder-containing CuNW film in CuNW/GCE with binder materials being indicated by arrows

In order to compare the electron transfer resistance between F-CuNWE and CuNW/GCE, the electrochemical impedance spectra (EIS) of two electrodes were recorded. In EIS, a linear portion at low frequencies is associated with a diffusion limited electrochemical process and a semicircle portion at high frequencies is related to an electron transfer limited process. Fig. 3(a) presents the impedance spectra obtained in the form of Nyquist plots, which were fitted based on the Randles equivalent circuit as shown in Fig. 3(b). This equivalent circuit consists of the ohmic resistance of the electrolyte solution (R1), the charge transfer resistance (R2), the Warburg impedance (W1) and the double layer

capacitance (Cl). The obtained values of R2 for F-CuNWE and CuNW/GCE are, respectively, about 3.5 Ω and 90.7 Ω, indicating that the electron transfer at the F-CuNWE is much faster than that at the CuNW/GCE. The very low electron transfer resistance observed in F-CuNWE can be attributed to the fact that CuNWs serve as both conductive substrate and electrocatalyst and thus can overcome the drawbacks resulting from the use of polymer binder and the presence of substrate-electrocatalyst interface. In addition, the double layer capacitance ratio between F-CuNWE and CuNW/GCE obtained by the fitting is about 24.3. This implies that the electrochemical active surface area of the F-CuNWE should be much higher than that of the CuNW/GCE.
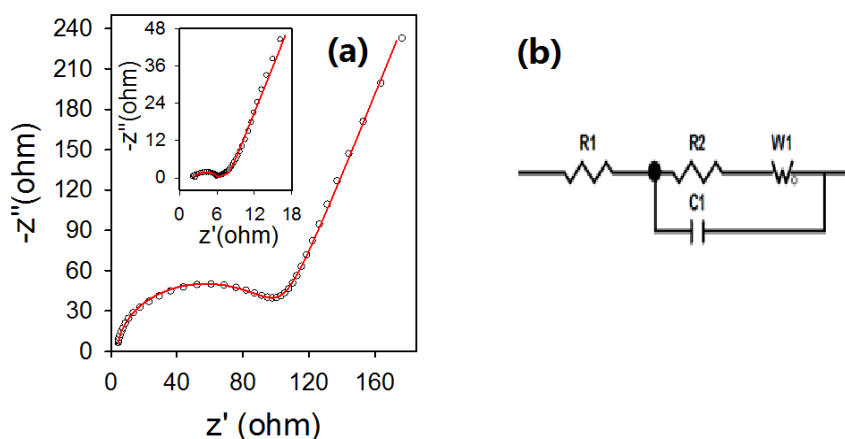

Figure 3. (a) Electrochemical impedance spectra (open circles) of the CuNW/GCE recorded in 0.1 M KCl solution containing 0.01 mM [Fe(CN)6]3-/4-. Inset is the impedance spectra of the F-CuNWE. The red curves were the fitting curves based on the Randles equivalent circuit (b).

3.2 Electroreduction of 4-NP at different Cu electrodes

To clarify the effect of both charge transfer and active surface area on the reduction of 4-NP, three types of Cu electrodes, namely polished Cu wire electrode with fast charge transfer but low active surface area, CuNW/GCE with slow charge transfer but relatively higher active surface area compared to the Cu wire electrode and F-CuNWE with fast charge transfer and high active surface area, were studied by cyclic voltammetry (CV). At the Cu wire electrode, no well-defined peak associated with the reduction of 4-NP appears in the potential window of -0.2 to -0.8 V (vs. SCE), irrespective of the concentration of 4-NP used (Fig. 4a). At the CuNW/GCE (Fig. 4b), however, we can observe a well-defined peak with its current increasing as the 4-NP concentration increases, indicating that this peak is related to the reduction of 4-NP. These observations hint that although the electron transfer is fast at the Cu wire electrode, its low active surface area leads to a very low 4-NP consumption rate and is thus responsible for the lack of reduction peak in the CV scan. As shown in Fig. 4c, a well-shaped peak associated with the reduction of 4-NP can be also observed at the F-CuNWE. However, a close examination of the reduction peaks observed at two types of CuNW electrodes reveals several significant differences. (i) The reduction peaks at the CuNW/GCE are broad and asymmetrical, especially in the case of high 4-NP concentrations. By contrast, the reduction peaks

at the F-CuNWE look more narrow and symmetrical, regardless of whether the concentration of 4-NP is high or low. (ii) The peak potential at the F-CuNWE is positively shifted in comparison with that at the CuNW/GCE, hinting that the reduction of 4-NP at the F-CuNWE is easier. (iii) For a given 4-NP concentration, the peak current observed at the F-CuNWE is more than 30 times higher than that at the CuNW/GCE. The differences observed should be related to the fact that compared with the CuNW/GCE, the F-CuNWE not only has a much lower electron transfer resistance but also possesses a higher active surface area originating from its porous network structure. These observations also suggest that the F-CuNWE owns a much higher catalytic activity for electroreduction of 4-NP in comparison with the CuNW/GCE.
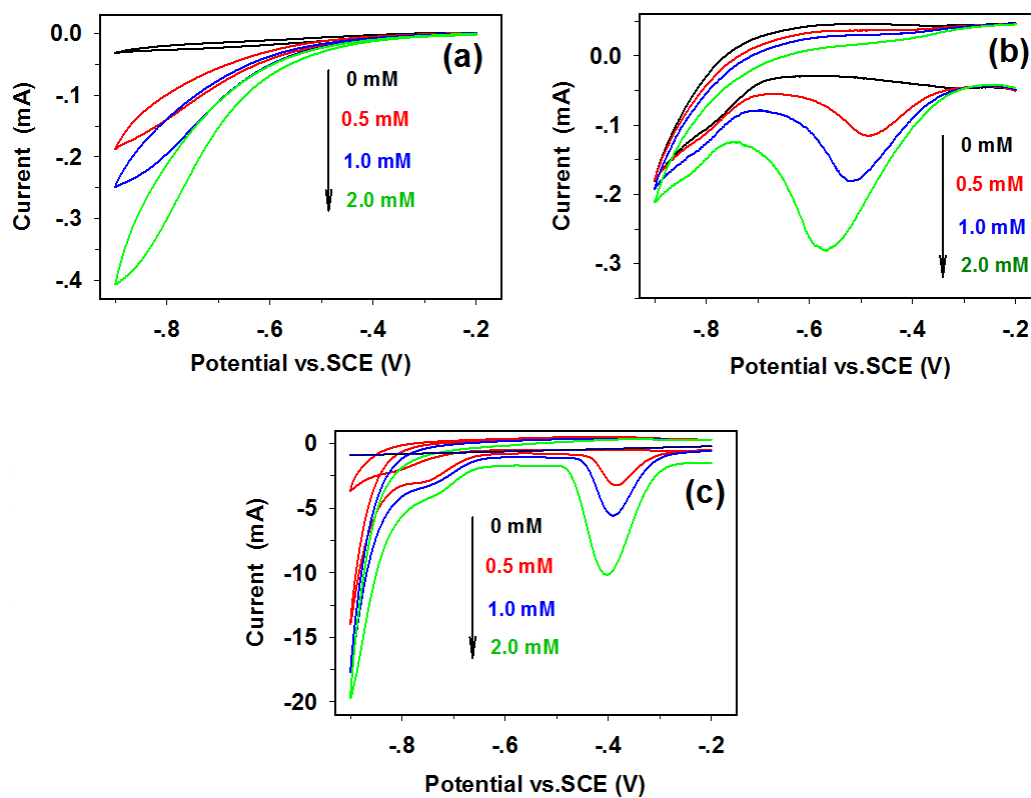

Figure 4. CV curves recorded at different electrodes in an acetate buffer solution in the absence or presence of 4-NP (pH=5): (a) Cu wire electrode of 1.5 mm in diameter and 1.0 cm in length, (b) CuNW/GCE, and (c)F-CuNWE. The scan rate is 50 mV s^{-1}.

Besides the reduction peak in the potential window of -0.2 to -0.6 V, which is commonly attributed to the reduction of –NO$_2$ to –NHOH, a shoulder peak in the potential range of -0.6 to -0.8 V can be also observed at the F-CuNWE. This peak should be related to the reduction of –NHOH to –NH$_2$ (this reduction peak cannot be observed at the CuNW/GCE probably due to the overlapping with the peak associated with the reduction of –NO$_2$ to –NHOH). However, no oxidation peak is visible in the reverse scan. In addition, the current of the reduction peak (i_p) in the potential range of -0.2 to -0.6 V increases with the square root of the scan rate (see Fig. 5). These results imply that the reduction of 4-NP at the F-CuNWE is an irreversible, diffusion-controlled process.
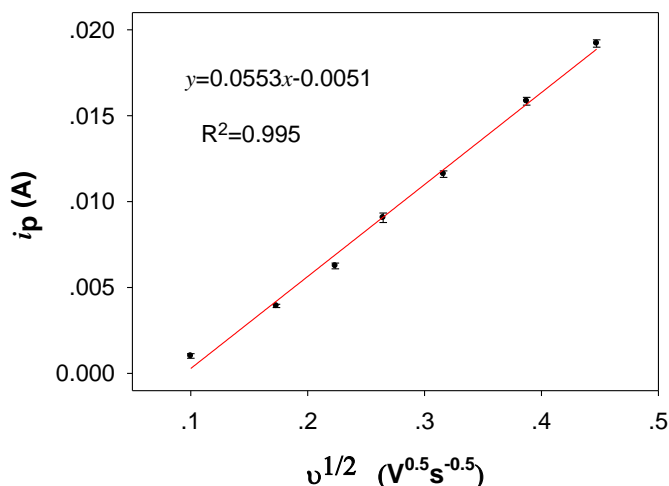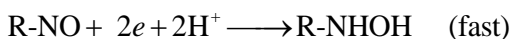
Figure 5. Plot of the current of the reduction peak (i_p) in the potential range of -0.2 to -0.6V observed at the F-CuNWE as a function of the square root of the scan rate (4-NP concentration is 1 mM). The straight line is the linear fitting. The error bars indicate the standard deviation of triplicate measurements.

To understand the detailed reduction mechanism observed in the potential window of -0.2 to -0.6 V, the number of electrons transferred in the rate-determining step (n_α) is evaluated. The value of n_α is obtained by Eq. 1 [22].

$$\alpha \cdot n_\alpha = 47.7/(E_P - E_{P/2}) \qquad (1)$$

where α, E_p and $E_{p/2}$ are the charge transfer coefficient, peak potential and half-height potential, respectively. Since α is generally assumed to be 0.5 in a totally irreversible electrode process [22], n_α is calculated to be about 2 by using $E_p = 390$ mV and $E_{p/2} = 341$ mV in the case of 1 mM 4-NP present in the solution (see Fig. 4c). Based on the result that the rate-determining step is a two-electron step, a possible reduction mechanism in the potential window of -0.2 to -0.6 V at the F-CuNWE is proposed as follows.

$$\text{R-NO}_2 + 2e + 2\text{H}^+ \longrightarrow \text{R-NO} + \text{H}_2\text{O} \quad \text{(slow, rate-determining step)}$$

$$\text{R-NO} + 2e + 2\text{H}^+ \longrightarrow \text{R-NHOH} \quad \text{(fast)}$$

3.3 Electrochemical detection of 4-NP

The performance of the F-CuNWE as a 4-NP sensor was also examined by a simple electrochemical technique (namely CV), and the reduction peak associated with the reduction of –NO$_2$ to –NHOH was chosen as the indicator for detection of 4-NP (Fig. 6a). It is obvious that this sensor can response well to the addition of 4-NP, either at low concentrations (e.g. several μM) or high concentrations (e.g. above 1 mM). The peak current is linearly related to the 4-NP concentration in the range of 4 to 2200 μM with a regression equation of I (mA)=4.831×10^{-3} C (μM) -0.5893 and a correlation coefficient R^2 of 0.997 (Fig. 6b). A sensitivity of 4.831 μA/μM is obtained from the slope

of the linear regression line. The limit of detection (LOD) of this sensor is obtained by LOD $=3\sigma/s$, where σ and s are the standard deviation of the blank signal and the sensitivity of the sensor, respectively. The value of LOD is calculated to be about 1.0 µM. The linear range, sensitivity and LOD of our sensor were compared with the Cu based sensors and some Ag or Au based sensors reported in the literature (Table 1). It is clear that our sensor not only possesses a lower detection limit but also has a much broader linear range and higher sensitivity than the reported porous Cu-modified GPE [17]. Moreover, in comparison with most of Ag or Au-based sensors, our Cu-based sensor also owns its advantages: a higher sensitivity and a broader linear range up to 2200 µM, with its detection limit being comparable to some Ag or Au-based sensors, e.g. Au/GCE [10], Ag-MCNT/GCE [15], Au amalgam/Au disc [9], Ag amalgam electrode [8] and Au-graphene/GCE [13].
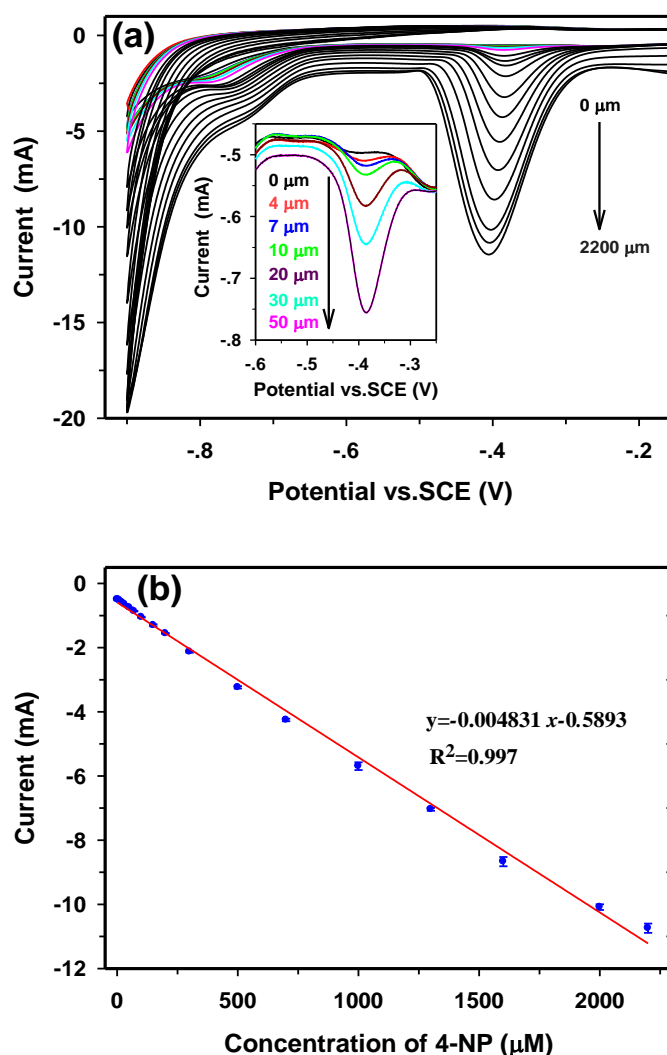

Figure 6. (a) CV curves recorded at the F-CuNWE with a scan rate of 50 mV s−1 in an acetate buffer solution containing different concentrations of 4-NP (pH=5) with the inset being an enlarged version at low 4-NP concentrations and (b) plot of peak current against 4-NP concentration with the straight line being its linear fitting. The error bars indicate the standard deviation of triplicate determinations for each concentration of analyte.

Table 1. Comparison between the performances of Cu, Ag, and Au-based sensors for 4-NP detection

Electrode materials	Analytical method	Linear range (μM)	Sensitivity (μA/μM)	LOD (μM)	Correlation coefficient R^2	Refs.
Au-graphene/GCE	Amperometry	470-10075	0.0523	0.47	0.9943	13
Au-RGO/GCE	Differential pulse votammetry	4-100 0.05-2	0.11 2.29	— 0.01	0.9975 0.9981	14
Au amalgam /Au disc	square wave voltammetry	5-250	0.01	1	0.9975	9
Au/GCE	Semiderivative voltammetry	10-1000	—	8	—	10
Ag-MCNT/GCE	LSV	3–120	2.88	1.3	0.9992	15
Ag-RGO/GCE	Amperometry	1-500	0.283	0.114	0.9981	16
Ag/GCE	Differential pulse votammetry	0.1-350	0.2055	0.015	0.9854	12
Ag amalgam electrode	Differential pulse votammetry	10-100	1.57×10^{-3}	1.5	0.993	8
Cu/GPE	Amperometry	50-850	0.1969	1.91	0.9997	17
Free-standing CuNW electrode	CV	4-2200	4.831	1.0	0.997	This work

To understand the anti-interference ability of our new Cu-based 4-NP sensor, the interference from several substances which were selected as the interfering materials in the detection of 4-NP at the Cu-modified GPE [17], namely phenol, 4-aminophenol, 4-bromophenol and 2,4-dichlorophenol, was investigated. The method of amperometry was used to study the response of F-CuNWE to these chemicals, in which phenol, 4-aminophenol, 4-bromophenol and 2,4-dichlorophenol at a level of 8 mM was successively injected before measuring the current response to 0.8 mM 4-NP. As illustrated in Fig. 7, it is clear that the amperometric response of our sensor to 0.8 mM 4-NP is not affected by the addition of 8 mM phenol, 4-aminophenol, 4-bromophenol or 2,4-dichlorophenol, indicating a good anti-interference ability of our sensor.
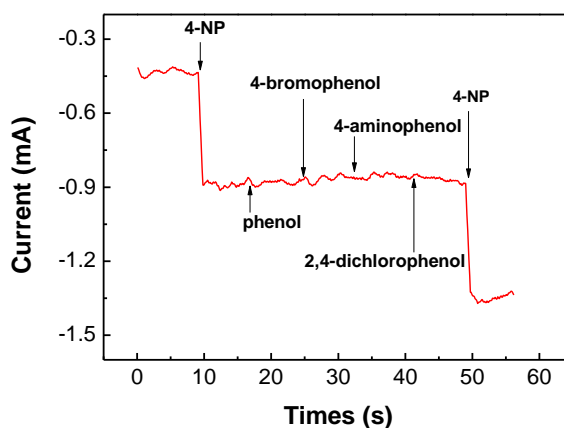

Figure 7. Amperometric responses of the F-CuNWE to successive additions of 4-NP (0.8 mM), phenol (8 mM), 4-bromophenol (8 mM), 4-aminophenol (8 mM), 2,4-dichlorophenol (8 mM) and 4-NP(0.8 mM) in an acetate buffer solution (pH=5). The applied potential was -0.4 V.

The stability and inter-electrode reproducibility of our sensor were also studied. When the F-CuNWE was stored under N_2 atmosphere at room temperature for 20 days, the response to 1 mM 4-NP still retained 93.7% of its original value, implying that the electrode can be used in long-term routine applications. To test the inter-electrode reproducibility, three F-CuNWEs were prepared, and their response to the reduction of 0.5 mM 4-NP was investigated by CV. The peak current recorded at these independent electrodes shows a relative standard of 4.8 %, indicating a good inter-electrode reproducibility.

The practical application of our new 4-NP sensor was tested by measuring the concentration of 4-NP in three samples. Sample 1 was the laboratory wastewater containing 4-NP in unknown quantity, whereas Sample 2 or Sample 3 was prepared by adding a given amount of 4-NP into tap water or river water (no 4-NP was detected in both tap water and river water before the addition of 4-NP). For comparison, the concentration of 4-NP was also measured by spectrometry. Table 2 shows a comparison between the results measured by two methods, as well as the recovery obtained by our sensor. It is obvious that the 4-NP concentration in each sample obtained by our sensor is close to that by spectrometry, with the relative differences for three samples being 4.8%, 1.5% and 1.4%, respectively. The recovery measured for Sample 2 or Sample 3 by our sensor is about 101.3 or 102.3%. These results suggest that our sensor can be used for detection of 4-NP in water.

Table 2. 4-NP concentrations of different samples measured by our sensor and by spectrometry

Water samples	Added (μM)	Found by our sensor (μM)	Found by spectrometry (μM)	Relative difference between two methods	Recovery by our sensor (%)
No. 1	—	45.7	43.5	4.8%	—
No. 2	440	445.7	439.1	1.5%	101.3
No. 3	35	35.8	35.3	1.4%	102.3

4. CONCLUSIONS

We have presented a study on the use of an F-CuNWE as the electrochemical sensor for detection of 4-NP. This new 4-NP sensor owns a porous network structure where CuNWs serve as both conductive substrate and electrocatalyst. EIS analysis reveals that the F-CuNWE has a much lower electron transfer resistance and a much higher active surface area in comparison with the CuNW/GCE. The fast electron transfer, along with high active surface area, makes the F-CuNWE more catalytically active for electroreduction of 4-NP than the CuNW/GCE. An investigation of this F-CuNWE as the 4-NP sensor by a simple electrochemical technique, namely CV, demonstrates that this new Cu-based 4-NP sensor exhibits a much better performance than the reported porous Cu-modified GPE. In addition, compared with most of Ag or Au based sensors, our Cu-based sensor also owns its advantages: a higher sensitivity and a broader linear range up to 2200 μM, with its detection limit being comparable to some Ag or Au-based sensors. To improve the detection limit of our sensor, the use of other electrochemical technologies for detection of 4-NP, e.g. differential pulse votammetry and square wave voltammetry, will be considered in our future work.

References

1. V. Uberoi and S.K. Bhattacharya, *Water Environ. Res.*, 69 (1997) 146.
2. M. Megharaj, H.W. Pearson and K. Venkateswarlu, *Pesticide Biochem. Physiol*,. 40 (1991) 266.
3. J.A. Brecken-Folse, F.L. Mayer, L.E. Pedigo and L.L. Marking, *Environ. Toxicol. Chem.*, 13 (2010) 67.
4. Agency for Toxic Substances and Disease Registry (ATSDR), Toxicological Profile for Nitrophenols 1992,1.
5. M.Wu and X. S. Zhu, *Chinese J. Anal. Chem.*, 37 (2009) 1691.
6. X. Liu, Y. Ji, Y. Zhang, H. Zhang and M. Liu, *J. Chromatogr. A*, 1165 (2007) 10.
7. J. Liu, H. Chen, Z. Lin and J.M. Lin, *Anal. Chem.*, 82 (2010) 7380.
8. A. Danhel, B. Yosypchuk, V. Vyskocil, J. Zima and J. Barek, *J. Electroanal. Chem.*, 656 (2011) 218.
9. F. Afzali, M.H.A. Zavar, G. Rounaghi and N. Ashraf, *Electrochim. Acta*, 209 (2016) 654.
10. L. Chu, L. Han and X.L. Zhang, *J. Appl. Electrochem.*, 41 (2011) 687–694.
11. A. Danhel, V. Mansfeldova, P.Janda, V. Vyskocil and J. Barek, *Analyst,* 136 (2011) 3656.
12. C. Karuppiah, S. Palanisamy, S.M. Chen, R. Emmanuel, M.A. Ali, P. Muthukrishnan, P. Prakash and F.M.A. Al-Hemaid, *J. Solid State Electrochem.*, 18 (2014) 1847.
13. W.B. Zhang, J.L. Chang, J.H. Chen, F. Xu, F. Wang, K. Jiang and Z.Y. Gao, *Res. Chem. Intermed.*, 38 (2012) 2443.
14. Y.H. Tang, R. Huang, C.B. Liu, S.L. Yang, Z.Z. Lu and S.L. Luo, *Anal. Methods*, 5 (2013) 5508.
15. B.Z. Liu, T. Wang, C.T. Yin and Z.L. We., *J. Mater. Sci.*, 49 (2014) 5398.
16. G.Q. Yang, *Int. J. Electrochem. Sci.*, 10 (2015) 9632.
17. A.N. Kawde and M.A. Aziz, *Electroanal.*, 26 (2014) 2484.
18. P. Zhang, Y. Sui, G. Xiao, Y. Wang, C. Wang, B. Liu, G. Zou and B. J. Zou, *J. Mater. Chem. A*, 1 (2013) 1632-1638.
19. J.H. Liang, Y.F. Zheng and Z.J. Liu, *Sensors Actuat. B*, 232 (2016) 336.
20. A. R. Rathmell and B. J. Wiley, *Adv. Mater.*, 23 (2011) 4798.
21. Y.F. Zheng, J.H. Liang, Y.Y. Chen and Z.J. Liu, *RSC Adv.*, 4 (2014) 41683.
22. A.J. Bard and L.R. Faulkner, Electrochemical Methods Fundamentals and Applications, John Wiley & Sons, Inc., (2005) New York, USA.